

arch-ive/9809019
ILL-(TH)-98-#14
August, 1998

**Abelian Links, Monopoles, and Glueballs
in $SU(2)$ Lattice Gauge Theory**

John D. Stack and Rafal Filipczyk

*Department of Physics
University of Illinois at Urbana-Champaign
1110 W. Green Street
Urbana, IL 61801*

PACS Indices: 11.15.Ha
12.38.Gc

Abstract

We investigate the masses of 0^+ and 2^+ glueballs in $SU(2)$ lattice gauge theory using abelian projection to the maximum abelian gauge. We calculate glueball masses using both abelian links and monopole operators. Both methods reproduce the known full $SU(2)$ results quantitatively. Positivity problems present in the abelian projection are discussed. We study the dependence of the glueball masses on magnetic current loop size, and find that the 0^+ state requires a much greater range of sizes than does the 2^+ state.

1 Introduction

The attempt to understand confinement in QCD has continued ever since Gell-Mann and Zweig introduced the quark concept. Attention has focussed almost universally on the pure gauge theory without light dynamical quarks as the place to begin study of the non-perturbative physics involved in confinement. In the absence of light dynamical quarks, what is meant by confinement can be precisely defined. Namely, in a confining theory, Wilson's loop must show an area law, or what is equivalent, the fundamental string tension must be finite.

Having simplified full QCD to pure $SU(3)$ gauge theory, many theorists have gone one step further and simplified to pure $SU(2)$ gauge theory. The physics of confinement is thought to be quite similar for any of the $SU(N)$ groups, of which the simplest is $SU(2)$. While an $SU(2)$ gauge theory obviously cannot explain the spectrum of baryons, lattice gauge theory simulations have shown that the meson spectra of pure $SU(2)$ and $SU(3)$ gauge theories are remarkably alike.

A major effort has been devoted to the theoretical understanding of confinement in $SU(2)$ pure gauge theory, both in the continuum and on the lattice. Within this framework, the dominant theme has been to search for a topological explanation of confinement. Topological objects are postulated to dominate the Euclidean path integral and lead to an area law for Wilson loops. The topological objects usually considered are instantons, monopoles, and vortices. Of these, only instantons are firmly established semi-classically in Euclidean pure $SU(2)$ gauge theory. However, the general consensus of work done on instantons is that while they are surely highly relevant for understanding the breakdown of chiral symmetry in QCD, they appear to have little to do with confinement.

This leaves monopoles and/or vortices as possible agents of confinement in pure $SU(2)$ gauge theory. The present work is devoted to further exploring the monopole approach. Since the work of 't Hooft and Polyakov [1], monopoles are well-known to exist semiclassically if the gauge theory contains adjoint scalar fields in addition to the usual gauge fields. Such scalar fields are natural in $N=2$ supersymmetric $SU(2)$ gauge theory, and the famous work of Witten and Seiberg showed that non-perturbative phenomena in this theory are indeed driven by the 't Hooft-Polyakov monopoles present in the theory [2]. However, the relevance of the Witten-Seiberg work for understanding confinement in pure $SU(2)$ gauge theory remains uncertain.

The suggestion that monopoles nevertheless exist and control confinement in the pure non-abelian gauge theory was made much earlier by 't Hooft [3], who also advocated partial gauge-fixing as a way to see monopole physics more clearly. The basic physical picture of confinement via monopoles is the "dual superconductor", where the linear potential between heavy quark and anti-quark originates in a electric flux tube surrounded by the magnetic current of a monopole condensate. The fundamental string tension has been successfully calculated in this framework [4, 5]. The purpose of the present work is to see if the glueball spectrum can also be explained. Glueballs are as characteristic of a confining theory as the string tension, and any approach which purports to explain confinement should also produce quantitative results for the glueball spectrum.

To make the paper self-contained, the abelian projection formalism is reviewed in the next Section. The reader familiar with this can go immediately to Section 3. We will work in lattice units throughout, and since all states are even under charge conjugation in $SU(2)$ we will denote glueballs by their spin J and parity P as J^P .

2 The Abelian Projection

In 't Hooft's framework, the first step is a partial gauge-fixing, applied only to those gauge fields which are "charged", or have off-diagonal generators in the Lie algebra of the gauge group. The central idea is that the monopoles associated with the abelian gauge invariance left after partial gauge-fixing will control non-perturbative phenomena. For an $SU(2)$ gauge group with the generator T_3 diagonal, the gauge field A_μ^3 is the abelian field or "photon", and gauge-fixing is done only on $A_\mu^a, a = 1, 2$, or equivalently the charged fields

$$W_\mu^\pm = \frac{1}{\sqrt{2}}(A_\mu^1 \pm iA_\mu^2).$$

After gauge-fixing, the charged fields are ignored, the important physics being postulated to reside solely in the abelian gauge field and its monopoles.

The 't Hooft approach has been explored rather extensively in $SU(2)$ lattice gauge theory [6]. The maximum abelian gauge has been found to be the only form of the gauge-fixing condition which allows a quantitative abelian calculation of the string tension. In the continuum form of the maximum abelian gauge, the continuum functional

$$G_c \equiv \frac{1}{2} \sum_\mu \int ((A_\mu^1)^2 + (A_\mu^2)^2) d^4x = \sum_\mu \int (W_\mu^+ W_\mu^-) d^4x \quad (1)$$

is minimized over all $SU(2)$ gauge transformations, leading to the conditions

$$(\partial_\mu + igA_\mu^3)W_\mu^+ = (\partial_\mu - igA_\mu^3)W_\mu^- = 0,$$

where g is the $SU(2)$ gauge coupling.

Stated precisely the purpose of the present paper is to see if the glueball spectrum can also be explained in this gauge.

2.1 Lattice Gauge-Fixing

The $SU(2)$ lattice gauge theory is built out of link variables $U_\mu(x)$,

$$U_\mu(x) \equiv e^{iga\vec{A}_\mu \cdot \vec{\tau}},$$

where $\vec{\tau} = \vec{\sigma}/2$ are the generators of $SU(2)$ in the fundamental representation, and a is the lattice spacing. On the lattice, the maximum abelian gauge is obtained by maximizing the lattice functional

$$G_l = \sum_{x,\mu} \frac{\text{tr}}{2} [U_\mu^\dagger(x) \sigma_3 U_\mu(x) \sigma_3] \quad (2)$$

over all $SU(2)$ gauge transformations [7]. It is easy to show that in the continuum limit, maximizing G_l is equivalent to minimizing G_c .

The demand that G_l be stationary with respect to a gauge transformation at an arbitrary site y leads to the requirement that

$$X(y) \equiv \sum_{\mu} \left[U_{\mu}(y) \sigma_3 U_{\mu}^{\dagger}(y) + U_{\mu}^{\dagger}(y - \hat{\mu}) \sigma_3 U(y - \hat{\mu}) \right] \quad (3)$$

be diagonal. This can be accomplished by a gauge transformation $\Omega(y)$. However, the value of X at the nearest neighbors of y is affected by $\Omega(y)$, so the diagonalization of X over the whole lattice must be done iteratively.

It is useful to factor a $U(1)$ link variable from $U_{\mu}(x)$, writing $U_{\mu}(x) = u_{\mu}(x) w_{\mu}(x)$, where $u_{\mu}(x) = \exp(i\phi_{\mu}^3 \tau_3)$, and $w_{\mu}(x) = \exp(i\vec{\theta}_{\mu} \cdot \vec{\tau})$, with $\theta_{\mu}^3 \equiv 0$. The angle ϕ_{μ}^3 can be extracted from the matrix elements of U_{μ} by expanding the gauge-fixed $SU(2)$ link U_{μ} in Pauli matrices, writing

$$U_{\mu} = U_{\mu}^0 + i \sum_{k=1}^3 U_{\mu}^k \cdot \sigma_k. \quad (4)$$

Then $\phi_{\mu}^3 = 2 \cdot \arctan(U_{\mu}^3/U_{\mu}^0)$. The $SU(2)$ action is periodic in ϕ_{μ}^3 with period 4π . To carry over standard formulas from $U(1)$ lattice gauge theory, it is more convenient to use an angle $\bar{\phi}_{\mu}^3 \equiv \phi_{\mu}^3/2$, with $\bar{\phi}_{\mu}^3 \in (-\pi, \pi]$.

2.2 Monopole Location in $SU(2)$

The location of the magnetic current starts with plaquette angles $\bar{\phi}_{\mu\nu}^3$ constructed from $\bar{\phi}_{\mu}^3$,

$$\bar{\phi}_{\mu\nu}^3(x) = \partial_{\mu} \bar{\phi}_{\nu}^3 - \partial_{\nu} \bar{\phi}_{\mu}^3 = \bar{\phi}_{\mu}^3(x) + \bar{\phi}_{\nu}^3(x + \hat{\mu}) - \bar{\phi}_{\mu}^3(x + \hat{\nu}) - \bar{\phi}_{\nu}^3(x) \quad (5)$$

The plaquette angle $\bar{\phi}_{\mu\nu}^3$ is resolved into a Dirac string contribution, plus a fluctuating part:

$$\bar{\phi}_{\mu\nu}^3 = 2\pi \bar{n}_{\mu\nu} + \tilde{\phi}_{\mu\nu}^3, \quad (6)$$

where $\tilde{\phi}_{\mu\nu}^3 \in (-\pi, \pi]$ and $\bar{n}_{\mu\nu}$ is an integer [8]. The integer-valued magnetic current \bar{m}_{μ} is determined by the net flux of Dirac strings into an elementary cube:

$$\bar{m}_{\mu} = -\frac{1}{2} \epsilon_{\mu\nu\alpha\beta} \cdot \partial_{\nu} \bar{n}_{\alpha\beta}. \quad (7)$$

In the identification of \bar{m}_{μ} , elementary cubes were used, so a magnetic charge is located at the center of a spacial 1-cube, likewise for other components of the magnetic current. This is done mainly for practical reasons; if (say) 2-cubes were used instead, the effective lattice size would become 8^4 instead of 16^4 .

2.3 Abelian Wilson Loops

The maximum abelian gauge has in a global way made the charged link angles $\vec{\theta}_\mu$ as small as possible. Non-perturbative quantities are postulated to be solely contained in the abelian link angles ϕ_μ^3 or equivalently $\bar{\phi}_\mu^3$. This allows two abelian approximations to the full $SU(2)$ Wilson loop. In the first, we simply use the link angles $\bar{\phi}_\mu^3(x)$ in the standard $U(1)$ formula for a Wilson loop:

$$W_{U(1)} = \left\langle \exp \left(i \sum_x \bar{\phi}_\mu^3 J_\mu \right) \right\rangle, \quad (8)$$

where $\langle \cdot \rangle$ denotes the expectation value over the ensemble of $\bar{\phi}^3$ link angle configurations, and J_μ is an integer-valued current defined by the path of the heavy quark.

In $U(1)$ lattice gauge theory, a Wilson loop expressed as in Eq.(8) can be factored into a term arising from photon exchange, times a term arising from monopoles,

$$W_{U(1)} = W_{phot} \cdot W_{mon}. \quad (9)$$

The photon contribution is perturbative, so for non-perturbative quantities, the same information should be in W_{mon} as $W_{U(1)}$. The monopole Wilson loop W_{mon} forms our second abelian approximation to the full $SU(2)$ Wilson loop. An explicit formula for W_{mon} is obtained by writing J_μ as the curl of a Dirac sheet variable [9]; $J_\mu = \partial_\nu D_{\mu\nu}$, where ∂_ν denotes a discrete derivative. Then W_{mon} is given by

$$W_{mon} = \left\langle \exp \left(\frac{i2\pi}{2} \sum_x D_{\mu\nu}(x) F_{\mu\nu}^*(x) \right) \right\rangle_m, \quad (10)$$

where $\langle \cdot \rangle_m$ denotes the sum over configurations of magnetic current.¹ For a rectangular Wilson loop, a useful choice for the sheet variable $D_{\mu\nu}$ is to set $D_{\mu\nu} = 1$ on the plaquettes of the flat rectangle with boundary J_μ , and $D_{\mu\nu} = 0$ on all other plaquettes. In Eq.(10), $F_{\mu\nu}^*$ is the dual of the field strength due to the magnetic current; $F_{\mu\nu}^*(x) = \frac{1}{2} \epsilon_{\mu\nu\alpha\beta} F_{\alpha\beta}(x)$. The field strength itself is derived from a magnetic vector potential A_μ^m , $F_{\mu\nu} \equiv \partial_\mu A_\nu^m - \partial_\nu A_\mu^m$, where

$$A_\mu^m(x) = \sum_y v(x-y) \bar{m}_\mu(y), \quad (11)$$

and \bar{m}_μ is the integer-valued, conserved magnetic current defined in Eq.(7).

To summarize, once we have gone to the maximum abelian gauge, our two abelian approximations to $SU(2)$ Wilson loops are Eq.(8) or Eq.(10). If the basic assumptions involved in the abelian projection are correct, non-perturbative quantities like the string tension and glueball spectrum should be obtainable from either one.

¹There is in principle a finite volume correction to Eq.(10) arising from Dirac sheets, [10], but we have checked that it is negligible in the present calculations.

3 Glueball operators

We will make use of standard methods for extracting the glueball spectrum in lattice gauge theory, as expounded in particular by Teper and collaborators [11]. The basic object of interest is Φ , called the glueball “wave function”. This is a gauge-invariant combination of $SU(2)$ links constructed so as to make $|\langle \Omega | \Phi | G \rangle|$ as large as possible, where $|\Omega \rangle$ is the $SU(2)$ vacuum, and $|G \rangle$ is a one glueball state, usually taken to have a definite three-momentum. In practice, Φ is a relatively simple Wilson loop-like combination of $SU(2)$ links, summed over orientations to project a definite spin-parity, and over spacial locations to project a definite three-momentum. An important advance made by Teper was to notice that $|\langle \Omega | \Phi | G \rangle|$ is numerically much larger if Φ is constructed out of “fuzzy” links [12]. Fuzzy links are constructed by replacing original products of two links in a given direction by themselves plus some fraction of “staples” (four-link products with the same endpoints as the original link). A related procedure applied directly to single links was introduced by the Ape collaboration [13]. This is commonly called “smearing”, and is what we use in the present work, when calculating with abelian links. To keep everything strictly local in Euclidean time, the staples used in smearing are spacial, *i.e.* for a z -link, the smeared staples are $x - z - x$ and $y - z - y$, but not $t - z - t$. Smearing is typically done several times in the full gauge theory [13], but here we smear the abelian links once, twice, or three times.

For the 0^+ and 2^+ glueballs, Φ is constructed out of simple rectangular Wilson loops, anchored at the spacial point \vec{x} , and lying in a particular spacial plane. The spin projection for 0^+ is done by averaging over the three spacial planes, $x - y$, $x - z$, and $y - z$, while for the 2^+ , the spin projection is accomplished by subtracting twice the $x - y$ rectangular loop from the sum of $z - x$ and $z - y$ loops [11]. Projection to a three-momentum $\vec{p} = 0$ is done by summing over spacial points \vec{x} , divided by $N_x N_y N_z$, where N_x, N_y , and N_z are the number of lattice sites in x, y , and z -directions.

3.1 Glueballs and the Abelian Projection

In the present work, we evaluate the Wilson loops in the wave functions Φ either in terms of the abelian link angles $\bar{\phi}^3$ as in Eq.(8), or in terms of the magnetic current of monopoles as in Eq.(10). Using these, we calculate correlation functions which we label as

$$C(t)_{U(1)} = \langle \Phi(t)\Phi(0) \rangle_{U(1)} / \langle \Phi(0)\Phi(0) \rangle_{U(1)}$$

$$C(t)_{mon} = \langle \Phi(t)\Phi(0) \rangle_{mon} / \langle \Phi(0)\Phi(0) \rangle_{mon},$$

where t refers to the separation between the two time-slices where Φ is evaluated. Any vacuum expected value of Φ is assumed to have been removed. These calculations are analogous to calculating the potential using Eq.(8) and Eq.(10), respectively. The aim of course is to see if the glueball spectrum can be obtained in the maximum abelian gauge to a similar degree of accuracy as the string tension. The use of smeared links is straightforward in the calculation which uses abelian links directly, namely $C(t)_{U(1)}$,

and for this case we will report on our results both with and without smeared abelian links. The Wilson loops in the monopole correlation function are obtained by computing the dual flux through the surface of the loop. Calculating this flux through loops with smeared edges is somewhat complicated, so for the monopole correlation function we simply calculate directly using the simplest plane rectangular surface. In any case, after gauge-fixing to the maximum abelian gauge, smearing is not essential for obtaining good results, unlike the situation for full $SU(2)$. The process of going to the maximum abelian gauge and using either the resulting abelian links or monopoles results in correlation functions with much less noise than the full $SU(2)$ correlation functions.

3.2 Positivity

The full $SU(2)$ correlation function $C(t)_{SU(2)}$ is of the form

$$C(t)_{SU(2)} = \sum_i c_i \cdot e^{-E_i t} \quad (12)$$

where we again assume any vacuum expected value of Φ has been removed, and for simplicity treat the case of a system finite in space but infinite in time. Since $C(t)_{SU(2)}$ is normalized to 1.0 at $t = 0$, we have

$$c_i = |\langle \Omega | \Phi | i \rangle|^2 / \sum_i |\langle \Omega | \Phi | i \rangle|^2,$$

so the non-zero coefficients c_i are positive and certainly less than unity. On a lattice with finite time extent and periodic boundary conditions, we must make the replacement $e^{-E_i t} \rightarrow e^{-E_i t} + e^{-E_i(T-t)}$ in Eq.(12) to satisfy periodicity. In addition, a constant b , independent of t but of order $\exp -T$ will in general be present in the correlation function [14]. It is easy to show that for an $SU(2)$ action with nearest neighbor couplings in time and a positive transfer matrix, the coefficients c_i continue to be positive and < 1.0 . Our calculations were done with the Wilson $SU(2)$ action, which satisfies the above properties.

The correlation function $C(t)_{U(1)}$ is obtained by replacing each $SU(2)$ link in Φ by its $U(1)$ approximation in the maximum abelian gauge. The correlation function $C(t)_{mon}$ involves a further approximation in which only the contributions of monopoles are retained, and photons or abelian gluons are dropped.

The correlation functions $C(t)_{U(1)}$ and $C(t)_{mon}$ are fitted to a form [14]

$$b + c_0 \cdot (e^{-E_0 t} + e^{-E_0(T-t)}). \quad (13)$$

The fit is aimed at getting only the lowest energy eigenvalue, E_0 , in a given channel. The results show that the constant b is always very small, essentially zero, while the value of E_0 is generally in agreement within statistical errors with the corresponding full $SU(2)$ value.

Problems with positivity show up in two ways. The first has to do with the constant c_0 . In the full $SU(2)$ correlation function a good choice of the operator Φ will generally increase the value of c_0 , but positivity always requires $c_0 < 1.0$. However in $C(t)_{mon}$ and

$C(t)_{U(1)}$, fits of the form of Eq.(13) do result in $c_0 > 1.0$. The problem is more severe for $C(t)_{mon}$ where values of $c_0 > 1.3$ are common.

The second difficulty is that an acceptable fit of the form Eq.(13) is often not possible without dropping small t points, $t = 0, 1$, or in some extreme cases $t = 0, 1, 2$. This could happen for a function which does satisfy positivity, if the lowest eigenvalue E_0 is not sufficiently dominant. In such a case, the 'effective eigenvalues'

$$E_0(t) \equiv -\ln(C(t+1)/C(t))$$

will *decrease* with increasing t , reflecting the fact that the exact correlation function of the form Eq.(12), is concave upward. The failure of the fit to a simple exponential would in this case merely represent the importance of physical excited states in the correlation function. However for $C(t)_{U(1)}$ and $C(t)_{mon}$, it is often true that the values of $E_0(t)$ *increase* with t for $t = 0, 1$, showing that $C(t)_{U(1)}$ and $C(t)_{mon}$ violate this concavity requirement for small values of t . Our strategy for dealing with this problem violation is simple. We examine the effective eigenvalues $E_0(t)$ and look for a 'plateau'. If for small values of t , the $E_0(t)$ are *less* than those in the plateau, those values of t are omitted in the fit. The fit then runs from some t_{min} to $t=7$ on our 16^4 lattice. This procedure is of course heuristic, and is based on the assumption that for sufficiently large values of t , the true lowest eigenvalue of the underlying $SU(2)$ gauge theory will dominate in $C(t)_{U(1)}$ and $C(t)_{mon}$.

In a given channel, we use rectangular Wilson loops of various sizes as operators, and compute only diagonal terms, *i.e.* correlations of the same operator with itself. In the resulting fits, we favor results where the value of c_0 is as close to 1.0 as possible, that is we disfavor small c_0 since it implies that the operator has a small overlap with the state of interest, and we also disfavor values of c_0 much larger than 1.0 since they imply a large amount of positivity violation. Detailed examples will be given in the next section, where it will be seen that despite these problems with positivity, the final results are surprisingly reliable.

It is perhaps worth making some general comments as to why positivity violation occurs at all. Since we have a gauge system, a configuration of link angles on a given time-slice represents a physical configuration plus many redundant variables. One of the reasons for gauge-fixing is to reduce the number of irrelevant variables. However, as opposed to a gauge which acts on some local operator, putting a link angle configuration into the maximum abelian gauge is an iterative process, involving many sweeps of the lattice, and therefore coupling sites which are far apart on the lattice. While the non-locality thereby introduced must cancel out if only $SU(2)$ gauge-invariant operators are used, this is not true when links are represented only by their $U(1)$ parts. The effective action which generates $U(1)$ configurations in the maximum abelian gauge no longer has the properties of the original Wilson $SU(2)$ action, in particular, it will not be nearest-neighbor in time. Correlation functions can then violate standard positivity properties.

4 Calculations

4.1 Simulation and Gauge-Fixing

Our simulations were done on a 16^4 lattice, using the standard Wilson form of the $SU(2)$ action, at $\beta = 2.40$, and 2.50 . At each β , after equilibration, 2000 configurations were saved. Saved configurations were separated by 20 updates of the lattice, where a lattice update consisted of one heatbath sweep [15], plus one or two overrelaxation sweeps [16]. Each of these configurations was then projected into the maximum abelian gauge using the overrelaxation method of Mandula and Ogilvie, with their parameter $\omega = 1.70$ [17]. The overrelaxation process was stopped after the off-diagonal elements of $X(x)$ of Eq.(3) were sufficiently small. Expanding $X(x)$ in Pauli matrices,

$$X = X^0(x) + i \sum_{k=1}^3 X^k(x) \cdot \sigma_k, \quad (14)$$

we used

$$\langle |X^{ch}|^2 \rangle \equiv \frac{1}{L^4} \sum_x (|X^1(x)|^2 + |X^2(x)|^2) \quad (15)$$

as a measure of the average size of the off-diagonal matrix elements of X over the lattice, and required $\langle |X^{ch}|^2 \rangle \leq 10^{-10}$. This condition was reached in approximately 1000 overrelaxation sweeps. Even though our condition on $\langle |X^{ch}|^2 \rangle$ is very tight, the gauge-fixed configuration is not unique; Gribov copies can still occur. However, Hart and Teper have shown that the uncertainty in the string tension caused by the Gribov ambiguity is rather small [18]. We have assumed the same will hold for the glueball spectrum.

From each gauge-fixed $SU(2)$ link, the $U(1)$ link angle $\bar{\phi}_\mu^3$ was extracted using the formula $\bar{\phi}_\mu^3 = \arctan(U_\mu^3/U_\mu^0)$, as described in Section 1. Then making use of the plaquette angles $\bar{\phi}_{\mu\nu}^3$, the magnetic current $\bar{m}_\mu(x)$ was found.

4.2 The Glueball Spectrum in Maximum Abelian Gauge

In this section, we present our results for the glueball spectrum in detail. Our fits are all of the form Eq.(13). In Tables 1-8 below we present the data from our fits for the 0^+ and 2^+ channels at zero momentum for for abelian links and monopoles at $\beta = 2.50$, and $\beta = 2.40$. Since the three-momentum is zero, E_0 is in fact an estimate of the mass of the corresponding glueball, denoted as M_0 in the tables. The column labelled 'operator' labels the Wilson loop used in calculating $C(t)_{U(1)}$ or $C(t)_{mon}$. Thus in Table 1, the operator 2×1 means the correlation function involves a 2×1 Wilson loop correlated with itself, while the operator $(2 \times 1)_{-1}$ means a 2×1 loop smeared once, etc. The column labelled 'fit' lists the small t points omitted, if any, in the fit. The next column gives the fitted value of the coefficient c_0 in the fit, which we henceforth call the 'overlap'.

We have also studied (less extensively) the glueballs masses as derived from correlation functions with finite momentum. We took the momentum to be the lowest possible on

the lattice, $\pi/8$ in lattice units, in (say) the x -direction. The value of E_0 was derived from the corresponding correlation function in the same manner as for zero momentum. Then the mass M_0 was obtained by assuming the usual (continuum) relation between E_0 and M_0 ,

$$E_0 = \sqrt{M_0^2 + p^2}.$$

Representative finite momentum results at $\beta = 2.50$ are presented in Table 9.

Before presenting our final estimates of glueball masses, we first remark on some systematic trends which can be seen in the various tables. For data obtained from the link correlation functions (Tables 1-4), the overlap coefficient c_0 is safely within error bars of the physical range $0 < c_0 < 1$ for almost all cases. In contrast, for the monopole correlation functions (Tables 5-8), $c_0 > 1$ is the rule rather than the exception. Here we only find $c_0 < 1$ for the first few operators for the 2^+ state at $\beta = 2.50$. So for the link correlation functions, this gross violation of positivity is rather uncommon, while it is quite common for the data obtained from monopole correlation functions. Nevertheless, the values of E_0 given in the tables for the two cases indicate that link and monopole operators are coupling to the same set of states.

The need to drop small values of t from the fits to Eq.(13) is another indication of positivity violation, caused in each case by small values of the effective eigenvalues $E_0(t)$. This dropping of some points is always necessary when $c_0 > 1$, the extreme case being the 2^+ at $\beta = 2.5$ state from monopoles, where $c_0 > 1.4$ required dropping $t = 0, 1, 2$. However, for $c_0 < 1$, low effective eigenvalues for small t also necessitate dropping points at small t . The 2^+ at $\beta = 2.5$ state from monopoles also illustrates this.

We now turn in Table 10 to a comparison of our results for glueball masses with the best available full $SU(2)$ data. The latter is from Michael and Teper [19] who extracted glueball masses from 20,000 measurements at $\beta = 2.40$ on a 16^4 lattice, and 14,000 at $\beta = 2.50$ on a 20^4 lattice. Generally the agreement is good between monopoles and links and with the full $SU(2)$ results, especially for the lightest and heaviest states, namely the 0^+ at $\beta = 2.50$ and the 2^+ at $\beta = 2.40$. For the remaining states, there are some discrepancies at roughly the 5% level. This is not unreasonable, given the heaviness of glueballs vs. the square root of the string tension, and the relatively small number of measurements (2000) used in the present work.

4.3 Magnetic Current Loop Size and the Glueball Spectrum

In the maximum abelian gauge, the magnetic current can be resolved into closed loops containing different numbers of links. At $\beta = 2.50$, the percentage of magnetic current in loops containing less than 10, 20, 50 and 100 links is 43%, 51%, 56%, and 59%, respectively [4]. It has been known for some time that the fundamental string tension is unaffected by the small loops of magnetic current. At $\beta = 2.50$, dropping all current contained in loops with *less* than 100 links does not affect the string tension. On the other hand, if we increase the size of the smallest allowed magnetic current loop to 200 links, the resulting string tension is approximately 10% smaller than the correct value. So we can say that

loops ~ 100 links and larger are necessary to explain the $\beta = 2.50$ string tension.

In this section, we explore the dependence of the glueball spectrum on magnetic current loop size, discussing for simplicity only $\beta = 2.50$. For the 0^+ state, we will use 2×1 Wilson loops in $C(t)_{mon}$, for the 2^+ state, we will use 2×2 Wilson loops. The first question we asked is whether the masses are stable under the elimination of small magnetic current loops. We tested this by successively eliminating all loops with *less* than 10, 20, 50, 100 *etc.* links. If the glueball masses were to behave in the same manner as the string tension, the masses would be preserved up to a lower limit on sizes of ~ 100 links, but then would fall below their correct values. In fact the glueball masses behave somewhat differently than the string tension. For the 0^+ state, using the entire magnetic current, and the 2×1 Wilson loop in $C(t)_{mon}$, we obtained a mass of 0.72(2). While we obtain values consistent with this when we eliminate all magnetic current loops smaller than 6, 10, and 20 links, by the time we eliminate all loops containing less than 50 links, the 0^+ mass has fallen to 0.60(3), and steadily declines as we increase the size of the smallest loop of magnetic current allowed. Thus the 0^+ glueball state is sensitive to smaller loops of magnetic current than the string tension.

For the 2^+ state, using the entire magnetic current and the 2×2 Wilson loop in $C(t)_{mon}$, we obtained a mass of 0.98(8). We find that this mass is stable in successively eliminating loops of size less than 10, 20, 50, 100 links, and even somewhat beyond. (For the lower limit of 100 links, we obtained a mass of 0.98(2).) So the lower bound on sizes of loops of magnetic current needed to reproduce the 2^+ glueball is quite similar to that needed for the string tension.

Since glueball masses, like the string tension, are non-perturbative quantities, it might seem obvious that they would require the largest loops of magnetic current. The presence of these very large loops of magnetic current is thought to be a defining characteristic of a confining phase. For example, in $U(1)$ lattice gauge theory, they are present in the confining phase, and absent in the deconfined Coulombic phase [20]. To investigate this in the $SU(2)$ glueball spectrum, we tried extracting the masses from $C(t)_{mon}$ after eliminating all loops of magnetic current *larger* than a certain size. We find that the 0^+ and 2^+ states behave rather differently under these cuts. For the 0^+ , if the *upper* limit on loop sizes is taken to be 100 links, the resulting mass is close to the value obtained with the entire magnetic current, 0.75(3), *vs.* 0.72(2). However, upon raising the upper limit to 200 links, the mass is too small, 0.53(5), and remains so when the upper limit on loop size is raised still further giving 0.63(5) when the upper limit is 1000 links. Only when the upper limit is raised greater than 1000 links does the mass finally stabilize, reaching 0.70(8) by the time the largest loop of magnetic current contains 1500 links. Thus the 0^+ state is sensitive to the largest loops of magnetic current.

For the 2^+ , the story is different. When the upper limit on loop size is 100 links, the mass value obtained is too large, 1.48(6), *vs.* 0.98(8) obtained with the entire magnetic current. But by the time the upper limit is raised to 200 links, the mass is 1.05(15), and remains within error bars of 0.98(8) as the upper limit is raised steadily to 2000 links. So unlike the 0^+ and the string tension, explaining the 2^+ mass does not appear to require the largest loops of magnetic current.

In Table 11, we show 0^+ and 2^+ mass at $\beta = 2.50$ with various cuts on the number of links allowed in loops of magnetic current. In the Table, N_{min} denotes the number of links in the smallest allowed magnetic current loop, and N_{max} does likewise for the largest. There are two rather intriguing results. The first is the 0^+ state basically requires all of the magnetic current which resides in loops ≥ 50 links in size. (Note that this still means that over 50% of the current can be discarded.) The second is the relative insensitivity of the 2^+ state to the particular cut made on magnetic current. The 2^+ state is visible in a wide variety of windows, the exception being one which only allows small loops.

An interesting difference between 0^+ and 2^+ states has also been found in the work of Schäfer and Shurak [21] on instantons and glueballs. We now discuss the possible relation of their results to our own. In the instanton case, the 0^+ channel receives strong non-perturbative contributions from individual instantons and anti-instantons, as well as instanton-anti-instanton interactions. The 2^+ channel, on the other hand, does not receive contributions from individual instantons and anti-instantons, only a rather weak contribution from instanton-anti-instanton interactions. On the lattice, it is known that a distribution of instantons and anti-instantons, when cast into the maximum abelian gauge, is represented by a network of magnetic current [22], and a rough correspondence can be made between the size of an instanton and the size of the magnetic current loop it generates. Since instantons, anti-instantons and their interactions all give a non-perturbative contribution to the 0^+ correlation function, but only the interactions contribute to the 2^+ , it is natural for the 0^+ state to depend more strongly on magnetic current loops of all sizes than the 2^+ . While this conclusion is similar in the two approaches, our work would imply that the 0^+ still could not be quantitatively explained in an instanton gas/liquid, since the latter, having no confinement [23], contains too few of the very largest loops of magnetic current.

5 Conclusions and Summary

We have shown that contact can be made with the spectrum of glueballs in $SU(2)$ lattice gauge theory, using the maximum abelian gauge and computing correlation functions using either abelian links or monopoles. The calculations we have presented show rather convincingly that for sufficiently large values of t , both $C(t)_{U(1)}$ and $C(t)_{mon}$ are dominated by the lightest glueball in the channel of interest. The present calculations were done starting with 2,000 $SU(2)$ configurations, as opposed to the $O(20,000)$ used in conventional $SU(2)$ calculations. In addition, when glueballs are found using $C_{mon}(t)$, only the magnetic current is needed, which occupies around 1% (at $\beta = 2.50$) of the links on the lattice [4]. So despite the effort required to project a configuration into the maximum abelian gauge, the description finally involves a rather small subset of the variables in a full $SU(2)$ configuration. Further, the results on how different components of the magnetic current build up the 0^+ and 2^+ give information not readily obtainable in a conventional $SU(2)$ calculation.

Nevertheless, the present method of calculation; gauge-fixing, followed by a trunca-

tion of the degrees of freedom, is not a controlled approximation, and the results must be checked by comparing them with those from full $SU(2)$ calculations. One of the major uncertainties which shows up in the glueball calculations reported here is the presence of positivity violation. In calculations of the heavy quark potential, this was hardly visible at all. The only sign of it was a very small wrong sign Coulomb term seen in the potential calculated from monopoles [4]. No positivity violation was seen in the potential calculated with abelian links. In contrast, the glueball calculations done here show positivity violation occasionally with abelian links, and quite commonly with monopoles. It would clearly be of great interest to know the spectrum of masses which are allowed to appear in $C(t)_{U(1)}$ and $C(t)_{mon}$. If only physical states can occur, then positivity violation would imply that excited states may have coefficients with negative signs.² In this situation, standard upper bound statements on glueball masses are lost, but the spectrum still contains only physical states. In the maximum abelian gauge, the greatly reduced statistical errors of $C(t)_{U(1)}$ and $C(t)_{mon}$ vs $C(t)_{SU(2)}$ might make this a price worth paying.

We are interested in extending the present work in several directions. The first goal is to include the 0^- and 2^- , the next states up in mass in the $SU(2)$ glueball spectrum. Beyond this, we want to gather a much larger dataset to pin down any possible discrepancies between abelian link/monopole glueball masses and those obtained with full $SU(2)$, and finally attempt to extract excited state masses and compare those with full $SU(2)$. This could shed light on the allowed spectrum of $C(t)_{U(1)}$ and $C(t)_{mon}$, discussed above. The explanation of the glueball spectrum is clearly a challenge that any topological approach to confinement must meet.

This work was supported in part by the National Science Foundation under Grant No. NSF PHY 94-12556. During the early stages of this work, R. F. was supported in part by Department of Energy grant DE-FG02-91ER40677. The calculations were carried out on the Cray T-90 system at the San Diego Supercomputer Center at the University of California, San Diego, and the Power Challenge system at the National Center for Supercomputing Applications at University of Illinois, both supported in part by the National Science Foundation.

References

- [1] G. 't Hooft, Nucl. Phys. **B79**,276(1974), A. M. Polyakov, JETP Lett. **20**,194(1974).
- [2] N. Seiberg and E. Witten Nucl. Phys. **B426** 19 (1994).
- [3] G. 't Hooft Nucl. Phys. **B190**[FS3] 455 (1982).
- [4] J. D. Stack, S. N. Neiman, and R. J. Wensley, Phys. Rev. D **50** 3399 (1994).
- [5] G. S. Bali, V. Bornyakov, M. Muller-Preussker, and K. Schilling Phys Rev D **54** 2863 (1996).

²This happens in conventional calculations which use smearing and a cold-wall source [13].

- [6] See references in M. I. Polikarpov, Nucl. Phys. B (Proc. Suppl.) 53 (1997).
- [7] A. S. Kronfeld, M. Laursen, G. Schierholz, and U.-J. Wiese, Phys. Lett. B **198**,516(1987).
- [8] T. A. DeGrand and D. Toussaint, Phys. Rev. D **22**,2478,(1980).
- [9] P. A. M. Dirac, Phys. Rev. **74**,817(1948).
- [10] J. D. Stack, R. J. Wensley, and S. D. Neiman, Phys. Lett. B **385**, 261 (1996).
- [11] K. Ishikawa, G. Schierholz, and M. Teper Z. Phys. C 19 327 (1983).
- [12] M. Teper , Physics Letters B **183** 345 (1986).
- [13] The Ape Collaboration, Physics Letters B **192** 163 (1987).
- [14] F. Brandstaeter, A. S. Kronfeld, and G. Schierholz, Nucl. Physics **B345** 709 (1990).
- [15] M. Creutz, Phys. Rev. D **21**,2308(1980).
- [16] M. Creutz, Phys. Rev. D **36**,515(1987).
- [17] J. Mandula and M. Ogilvie, Phys. Lett. B **248**,156(1990).
- [18] A. Hart and M. Teper, Phys. Rev. D **55**, 3756 (1997).
- [19] C. Michael and M. Teper, Physics Letters B **199** 95 (1987).
- [20] See for example, R. J. Wensley and J. D. Stack, Phys. Rev. Lett. **63**,1764(1989).
- [21] T. Schäfer and E. V. Shuryak, Phys. Rev. Lett. **75** 1707 (1995).
- [22] A. Hart and M. Teper, Physics Letters B **371**, 261 (1996).
- [23] D. Chen, presentation at the International Conference on Lattice Field Theory, Boulder Colorado, July 1998.

Tables

Table 1: 0^+ state from abelian links at $\beta = 2.50$

operator	fit	c_0	M_0
2×1	0	0.81(2)	0.76(2)
$(2 \times 1)_{-1}$		0.99(1)	0.68(1)
2×2	0	0.91(2)	0.70(2)
$(2 \times 2)_{-1}$	0,1	1.15(8)	0.68(4)
3×2	0	0.92(2)	0.67(2)
3×3	0,1	1.04(7)	0.67(4)
4×4	0,1	1.04(7)	0.63(4)

Table 2: 2^+ state from abelian links at $\beta = 2.50$

operator	fit	c_0	M_0
3×3	0	0.63(2)	1.17(5)
$(3 \times 3)_{-1}$	0	0.95(3)	1.06(3)
$(3 \times 3)_{-2}$		0.992(5)	1.04(1)
4×4	0	0.62(6)	1.02(4)
$(4 \times 4)_{-1}$	0	1.05(3)	0.99(3)
5×5	0	0.55(2)	0.94(4)

Table 3: 0^+ state from abelian links at $\beta = 2.40$

operator	fit	c_0	M_0
1×1	0	0.93(3)	1.10(4)
$(1 \times 1)_{-1}$		0.94(3)	0.99(3)
2×1	0	0.99(3)	1.07(3)
2×2	0,1	1.2(2)	1.04(7)

Table 4: 2^+ state from abelian links at $\beta = 2.40$

operator	fit	c_0	M_0
2×2	0	0.67(9)	1.7(1)
$(2 \times 2)_{-1}$	0	0.86(8)	1.5(1)
3×3	0,1	0.73(6)	1.48(9)
$(3 \times 1)_{-1}$	0	0.7(1)	1.6(1)
$(4 \times 2)_{-1}$		1.00(1)	1.45(2)

Table 5: 0^+ state from monopoles at $\beta = 2.50$

operator	fit	c_0	M_0
2×1	0	1.19(2)	0.72(2)
2×2	0,1	1.38(9)	0.70(4)
3×1	0	1.19(2)	0.69(2)
3×3	0,1,2	1.9(4)	0.72(8)
4×4	0,1,2	2.0(4)	0.67(7)

Table 6: 2^+ state from monopoles at $\beta = 2.50$

operator	fit	c_0	M_0
2×2	0,1	0.9(1)	0.98(8)
3×1	0,1	0.6(1)	1.0(1)
4×1	0,1	0.7(1)	0.93(8)
5×1	0,1	0.7(1)	0.94(9)
3×2	0	1.21(3)	0.95(2)
3×3	0,1,2	1.4(5)	0.9(1)
4×4	0,1,2	1.8(6)	0.9(1)

Table 7: 0^+ state from monopoles at $\beta = 2.40$

operator	fit	c_0	M_0
1×1	0	1.33(4)	1.04(2)
2×1	0	1.34(3)	0.98(2)
2×2	0,1	1.6(1)	0.97(5)
3×1	0	1.34(3)	0.94(2)

Table 8: 2^+ state from monopoles at $\beta = 2.40$

operator	fit	c_0	M_0
2×2	0	1.39(7)	1.39(6)
3×1	0	1.35(7)	1.53(5)
4×1	0	1.25(6)	1.47(5)
5×1	0	1.23(8)	1.48(7)
6×1	0	1.17(8)	1.47(7)

Table 9: Finite momentum results from links and monopoles at $\beta = 2.50$

state	type	operator	c_0	M_0
0^+	links	2×1	0.81(2)	0.74(3)
2^+	links	4×4	0.66(3)	1.06(5)
0^+	monopoles	2×1	1.21(2)	0.66(2)
2^+	monopoles	2×2	1.24(4)	1.07(3)

Table 10: Glueball masses from full $SU(2)$, links, and monopoles

β	state	$SU(2)$	links	monopoles
2.5	0^+	0.72(3)	0.69(1)	0.70(1)
2.5	2^+	1.05(3)	1.04(1)	0.95(2)
2.4	0^+	0.94(3)	1.06(2)	0.99(1)
2.4	2^+	1.52(3)	1.47(2)	1.49(4)

Table 11: The 0^+ and 2^+ masses with cuts on the magnetic current

N_{min}	N_{max}	0^+	2^+
0	∞	0.72(2)	0.98(8)
20	∞	0.69(4)	1.00(2)
50	∞	0.61(3)	0.97(2)
100	∞	0.49(2)	0.98(2)
20	2000	0.69(5)	0.98(2)
20	1000	0.51(5)	1.00(3)
50	2000	0.61(5)	0.98(2)
100	1000	0.40(6)	0.96(3)
100	500	0.1(1)	0.95(4)

Figure Captions

Figure 1. The 0^+ correlation function from abelian links. Symbols:
diamonds – $(2 \times 1)_1$ loops, *crosses* – 2×2 loops , *squares* – 3×2 loops.

Figure 2. The 0^+ correlation function from monopoles Symbols:
diamonds – $(2 \times 1)_1$ loops, *crosses* – 2×2 loops , *squares* – 3×1 loops.

Figure 3. The 2^+ correlation function from abelian links. Symbols:
diamonds – $(3 \times 3)_1$ loops, *crosses* – $(4 \times 4)_1$ loops , *squares* – 4×4 loops.

Figure 4. The 2^+ correlation function from monopoles. Symbols:
diamonds – 2×2 loops, *crosses* – 3×2 loops , *squares* – 3×1 loops.

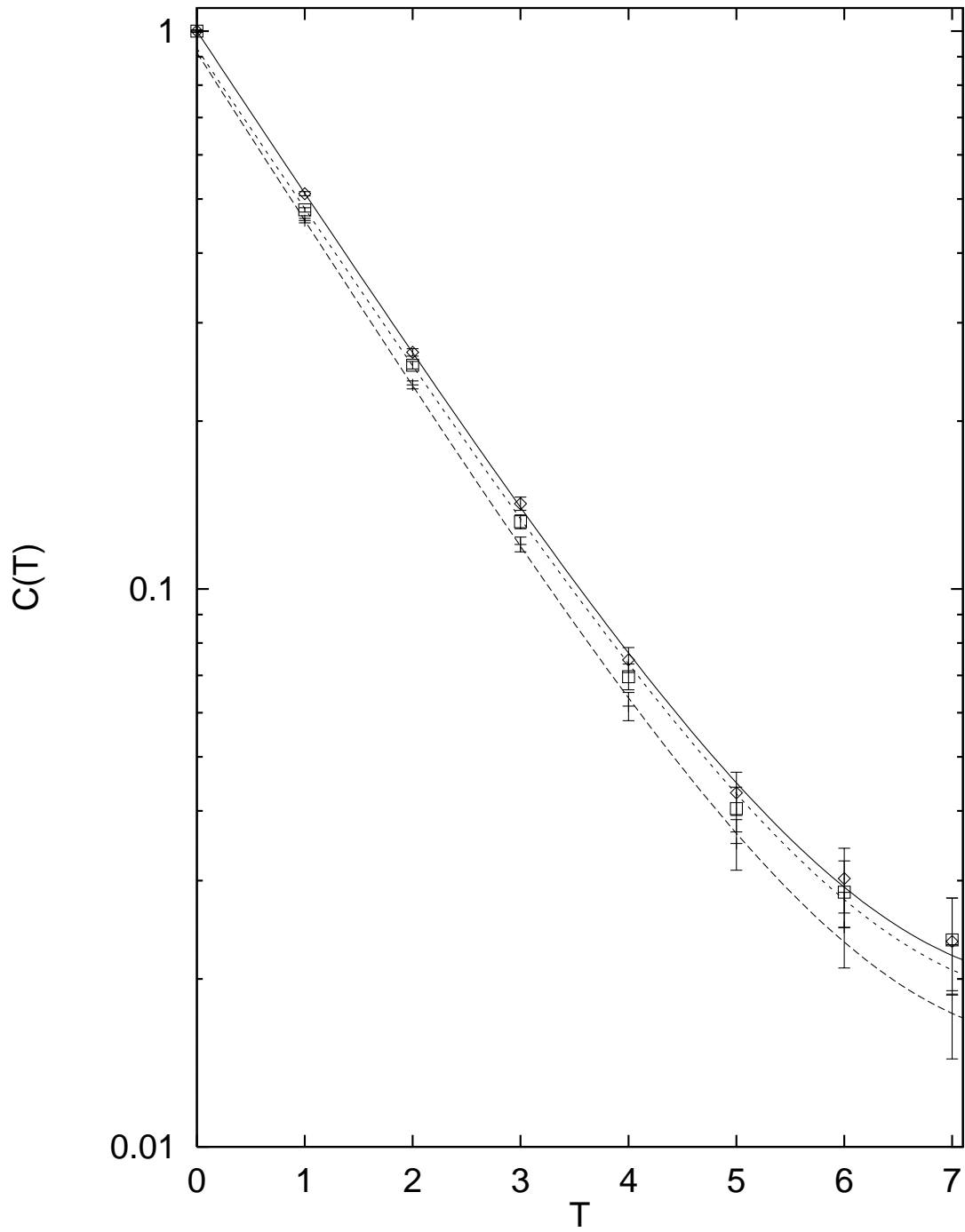


Figure 1

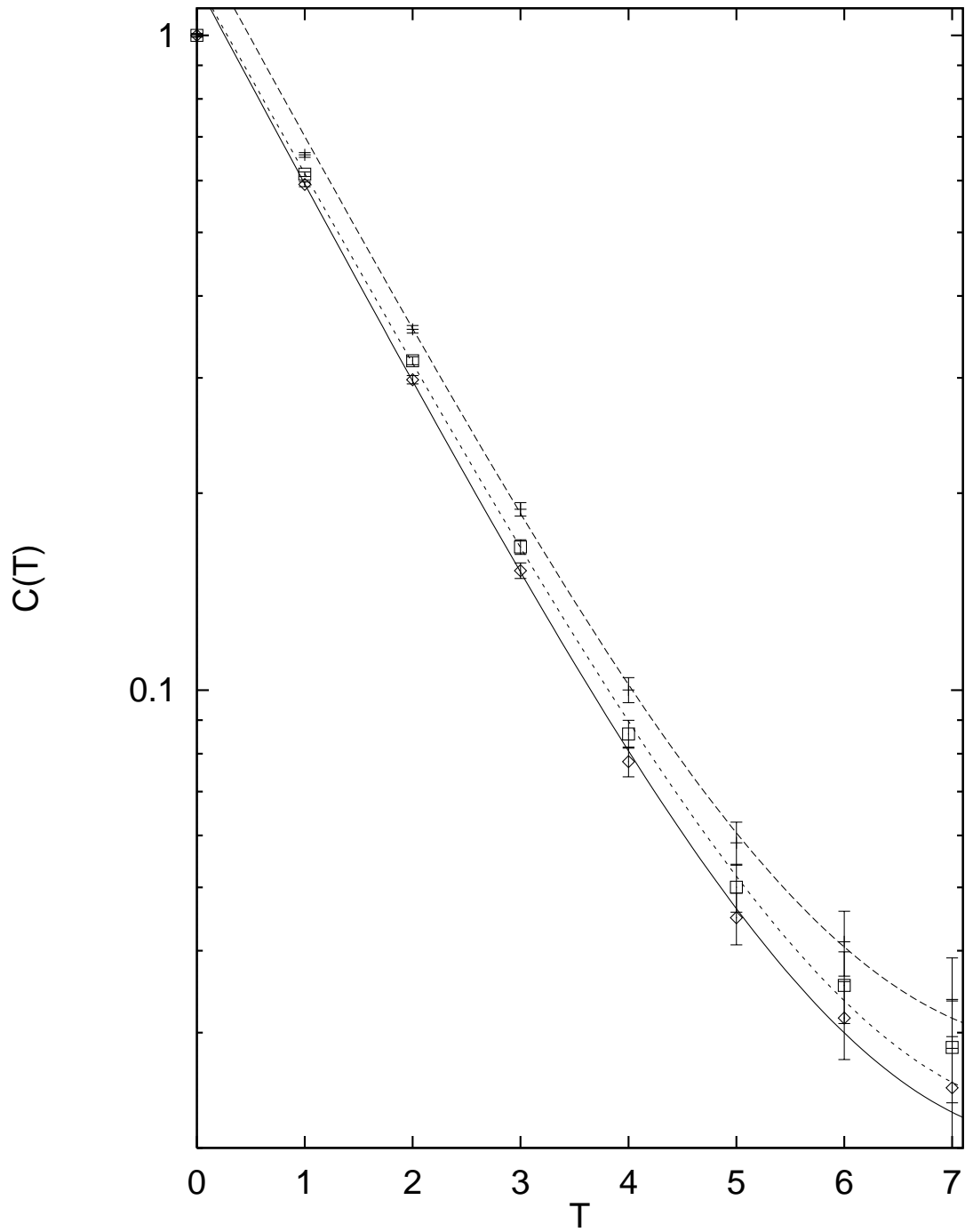


Figure 2

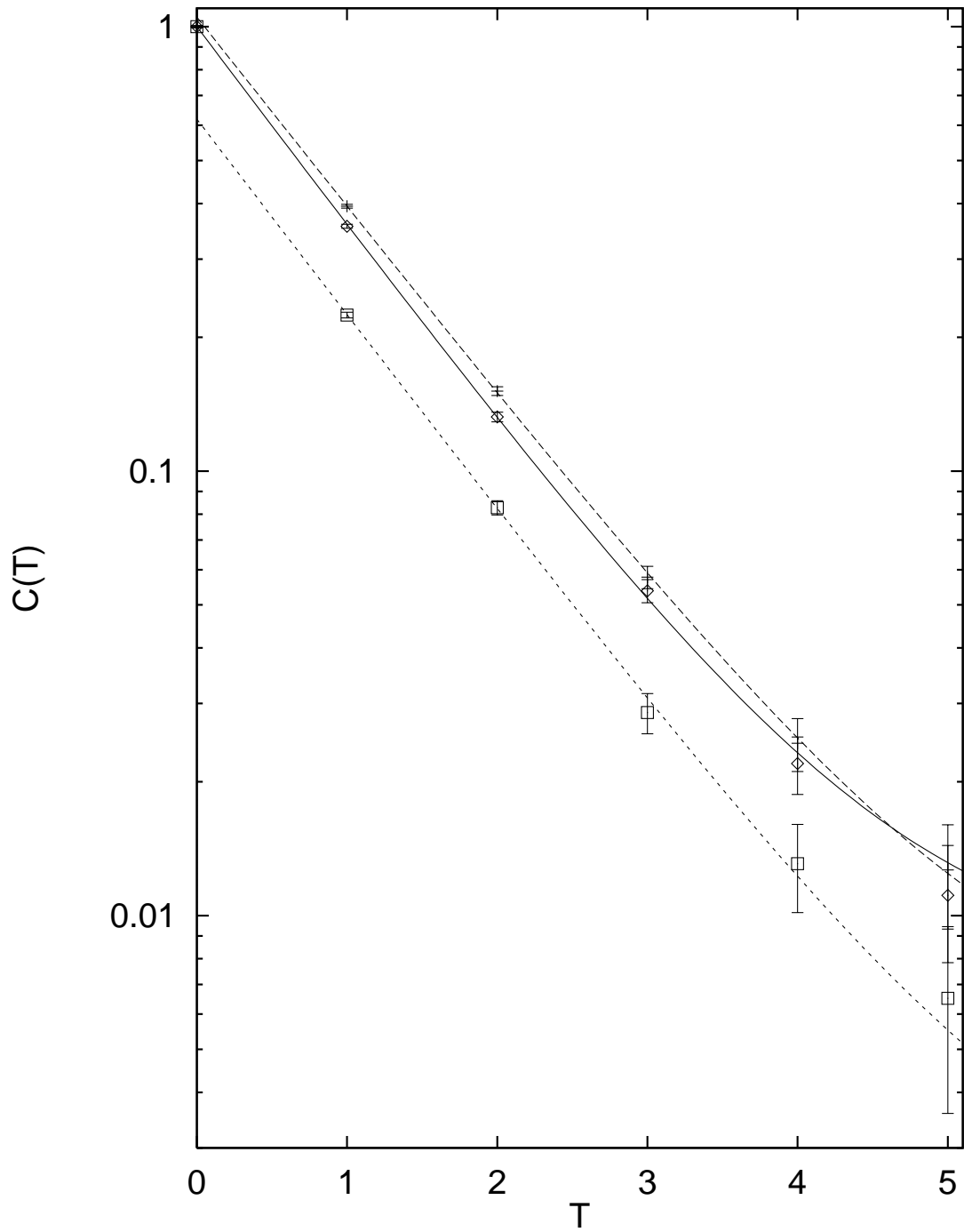


Figure 3

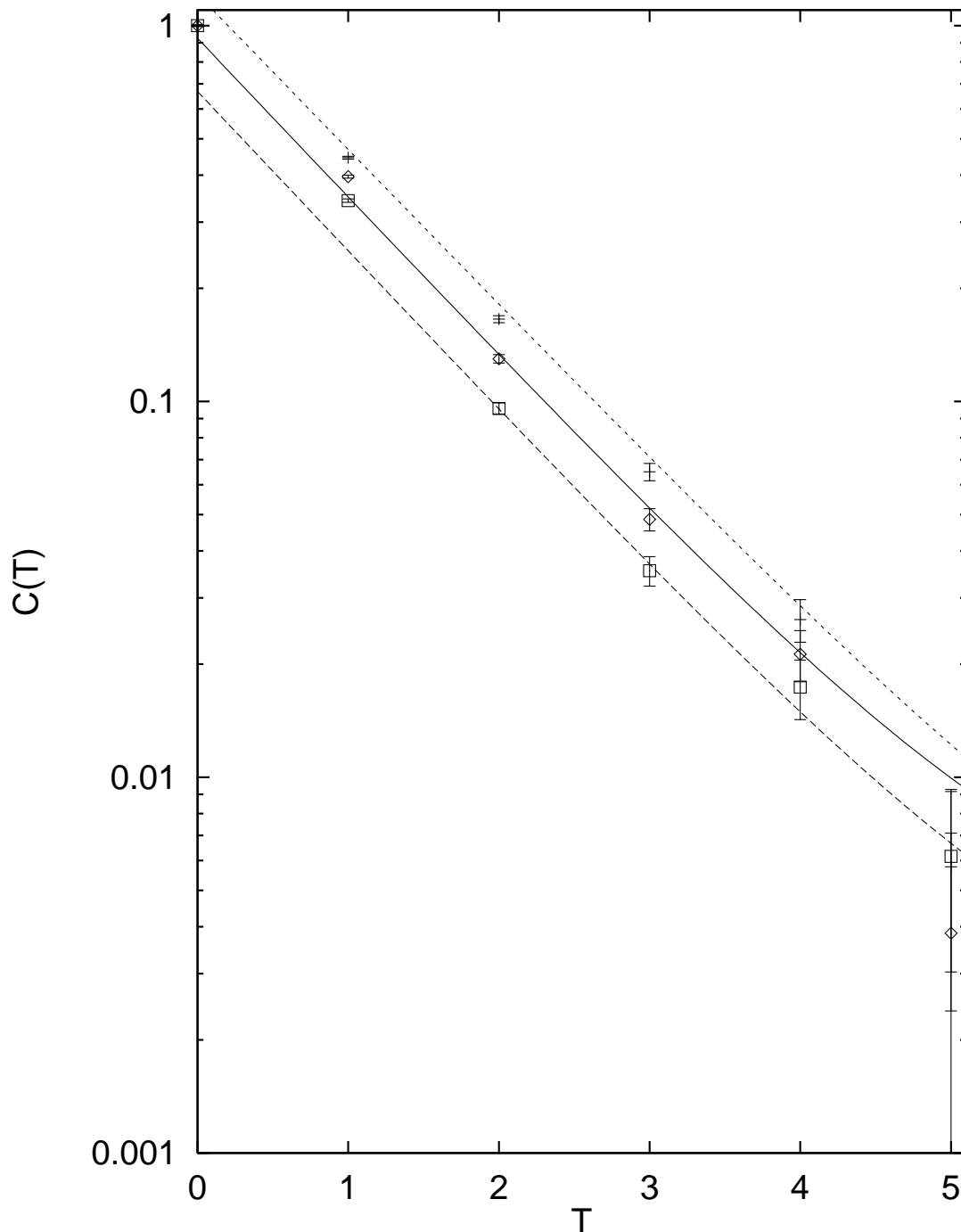


Figure 4